Med Biol Eng Comput (2016) 54:1229–1241
DOI 10.1007/s11517-015-1439-8

ORIGINAL ARTICLE

Hand–tool–tissue interaction forces in neurosurgery for haptic rendering

Marco Aggravi[1] · Elena De Momi[2] · Francesco DiMeco[3] · Francesco Cardinale[4] · Giuseppe Casaceli[4] · Marco Riva[5] · Giancarlo Ferrigno[2] · Domenico Prattichizzo[1]

Received: 11 December 2014 / Accepted: 12 December 2015 / Published online: 31 December 2015

Abstract Haptics provides sensory stimuli that represent the interaction with a virtual or tele-manipulated object, and it is considered a valuable navigation and manipulation tool during tele-operated surgical procedures. Haptic feedback can be provided to the user via cutaneous information and kinesthetic feedback. Sensory subtraction removes the kinesthetic component of the haptic feedback, having only the cutaneous component provided to the user. Such a technique guarantees a stable haptic feedback loop, while it keeps the transparency of the tele-operation system high, which means that the system faithfully replicates and render back the user's directives. This work focuses on checking whether the interaction forces during a bench model neurosurgery operation can lie in the solely cutaneous perception of the human finger pads. If this assumption is found true, it would be possible to exploit sensory subtraction techniques for providing surgeons with feedback from neurosurgery. We measured the forces exerted to surgical tools by three neurosurgeons performing typical actions on a brain phantom, using contact force sensors, while the forces exerted by the tools to the phantom tissue were recorded using a load cell placed under the brain phantom box. The measured surgeon–tool contact forces were 0.01–3.49 N for the thumb and 0.01–6.6 N for index and middle finger, whereas the measured tool–tissue interaction forces were from six to 11 times smaller than the contact forces, i.e., 0.01–0.59 N. The measurements for the contact forces fit the range of the cutaneous sensitivity for the human finger pad; thus, we can say that, in a tele-operated robotic neurosurgery scenario, it would possible to render forces at the fingertip level by conveying haptic cues solely through the cutaneous channel of the surgeon's finger pads. This approach would allow high transparency and high stability of the haptic feedback loop in a tele-operation system.

Keywords Haptic rendering · Contact forces · Brain phantom forces · Neurosurgery

✉ Marco Aggravi
aggravi@dii.unisi.it

Elena De Momi
elena.demomi@polimi.it

Francesco DiMeco
francesco.dimeco@istituto-besta.it

Francesco Cardinale
francesco.cardinale@ospedaleniguarda.it

Giuseppe Casaceli
gcasaceli@gmail.com

Marco Riva
mriva.eu@gmail.com

Giancarlo Ferrigno
giancarlo.ferrigno@polimi.it

Domenico Prattichizzo
prattichizzo@dii.unisi.it

[1] Department of Information Engineering and Mathematics, University of Siena, Via Roma 56, 53100 Siena, Italy

[2] Department of Electronics, Information and Bioengineering, Politecnico di Milano, Milan, Italy

[3] National Neurological Institute "C. Besta", Via Celoria 11, 20133 Milan, Italy

[4] "Claudio Munari" Epilepsy and Parkinson Surgery Centre, Niguarda Ca Granda Hospital, Piazza Ospedale Maggiore 3, 20162 Milan, Italy

[5] Unità of Oncological Neurosurgery Humanitas Research Hospital, Università degli Studi di Milano, via Manzoni 56, 20089 Rozzano, Italy

1 Introduction

Haptics refers to touch interactions and physical contacts during perception or manipulation of objects. Haptic rendering provides the user with sensory stimuli related to the virtual or tele-operated remote scenario, transmitting sensory information about the manipulated objects, or tissues [1]. Haptics is widely considered a valuable navigation and manipulation tool during tele-operated surgical procedures [2, 3]. In fact, it allows detecting local mechanical properties of the tissue being manipulated and distinguishing the presence of vessels [4, 5]. Moreover, force feedback has been shown to enhance operators' performance in tele-operation in terms of completion time of a given task [6], accuracy [7], and surgical safety [8]. Eventually, tele-operated systems with force feedback also allow recording the motions and forces, which can be used in training simulators [9, 10].

Visual and auditory feedback are easily replicable with screen and head-cuffs, but haptic feedback is less trivial to transmit [11]. To best render the touch sensation which occurs at the slave side of a tele-operation surgical system, understanding how haptic feedback can be provided to the operator is essential. Haptic sensation can be provided as cutaneous (tactile) and kinesthetic (force) information [12]. The former is represented by the pressure stimuli induced with skin deformation, whereas the latter concerns information coming from physical involvement of muscles. Tactile and kinesthetic perceptions have different thresholds, as described in physiology literature. Concerning the former, the sensitivity of the finger pads is best in the force range 0.05–3.5 N, [13]. In [14, 15], the authors determined the absolute threshold for touch force perception on the fingertip as being 0.8 mN, whereas in [16, 17] the threshold for the activation of an individual's pressure sensors ranges from 0.06 to 0.2 N per cm^2. Regarding kinesthetic perception, the overall mechanoreceptor system has a resolution of 0.06 N, with a differential threshold of 7 %, [18].

Achieving best performance for haptic rendering in tele-operated robotic surgery is equivalent to finding the best trade-off between having a system with high *transparency*, i.e., in which the tele-operated part of the system is able to faithfully replicate and render back the user's directives, and having a *stable* haptic feedback loop, where unwanted oscillations—which may be unsafe for the human operator and the remote environment—are filtered out, [19]. Stability issues result from communication latency in tele-operation, hard contacts, relaxed grasp of the user, and other destabilizing factors [20]. Such issues can be solved by reducing actuators at the user side, i.e., no force feedback is provided to the user end-effector, or by using appropriate control strategies. An approach for controlling the amount of kinesthesia introduced into the system by the human operator is called "sensory substitution." This term refers to those techniques which provide the brain with information coming from a sensory domain, typically visual information from the visual system and the eyes, by means of receptors and pathways of another sensory system, often represented by the skin and somatosensory system, [21]. Using sensory substitution techniques in the haptic loop of a tele-operation scenario was proved to be an intrinsically stable approach [22], because the human does not receive kinesthetic feedback from slave side of the tele-operation system.

Nevertheless, stability comes at a cost: a complete substitution of haptic sensations at the operator side drastically reduces the transparency of the system. One way to recover this loss is to feed only the cutaneous part of the haptic feedback to the operator. Since the kinesthetic component (which can lead to instability) is removed from the complete haptic feedback, this approach is stable as the sensory substitution technique. In [23], the authors coined the term "sensory subtraction" for referring to this approach, which is not a complete haptic substitution, in the sense that it keeps only the cutaneous part of the force feedback and removes the kinesthetic feedback. In the same work, the authors proved that, during tele-operated needle insertion, a cutaneous-only feedback approach allowed a shorter task completion time and a lower penetration beyond a set of virtual fixture, compared to a complete cutaneous and kinesthetic feedback approach. In [24], the authors decoupled the control of the two haptic interaction components by using a wearable cutaneous device together with a grounded haptic device. A grounded haptic display is an haptic device which is portable, but cannot be moved during its use, i.e., it is fixed during its usage [25]. In contrast, a wearable haptic device is usually lightweight and can be worn by the operator. They scaled down the kinesthetic component of the haptic feedback through the grounded interface, compensating this lack of force feedback with the cutaneous device. Compared to the lack of kinesthetic feedback, they obtained improved performance using such compensation technique and, in some conditions, performance comparable to the one registered while using the grounded interface alone.

In this work, we present a study focusing on tool contact forces and interaction forces with tissue during neurosurgery. Since the cutaneous perception range of the human finger pads is limited from 0 to 3.5 N—as shown by Lederman [13], if the interaction forces in play during neurosurgery are small enough to fit it, then we can render such forces as haptic feedback by using only the cutaneous channel of the fingertip. This would enable scenarios in which sensory subtraction techniques are used for tele-operated robotic neurosurgery. Our approach consisted of using contact force sensors to obtain the contact forces exerted by neurosurgeons to the surgical tools, whereas a

load cell placed under brain phantom measured the tool–tissue forces.

1.1 Related works

Although sensory subtraction and sensory substitution techniques could be efficiently employed in tele-operation scenarios—including robotic surgery—brain tissue mechanical characteristics make the haptic rendering a challenging task during neurosurgery [26, 27]. Chen et al. [28] measured penetration forces with a motor-driven force gauge apparatus while inserting a 3.0-mm ventricular shunt catheter at constant speed of 0.33 mm/s in a 0.6 % agarose gel phantom, 0.8 % agarose gel phantom, and in *in vivo* pig brain. The penetration transient is less than 0.1 N of insertion force for all the three cases studied. A recent study about the forces exerted on a cadaver brain tissue by robotic tele-operated arm during arachnoid dissection has been conducted by Marcus et al. [29], using a six DoF robotic system and a six DoF force/torque sensor placed at the end-effector. Measured forces exerted during carrying incision or tissue retraction were approximately 0.2 N, with low variability. Another interesting study has been proposed by Maddahi et al. [30], where the authors have conducted four operations in which the neuroArm surgical system [27] was employed to surgically remove brain tumors. The authors employed a bipolar forces and a suction tool, linked to the robot end-effector via two six DoF force/torque sensors. Regarding the interaction forces applied by the robot end-effectors to the brain tissue, the authors measured maximum force of 1.86 N, with mean values of $0.38\,\mathrm{N} \pm 0.05\,\mathrm{N}$ for the bipolar forceps and $0.21\,\mathrm{N} \pm 0.03\,\mathrm{N}$ for the suction tool. In [31], the authors fixed strain gauges between a probe mechanical advancer and two types of probes, i.e., a 2.5-mm stainless steel sphere and a standard 3.0-mm ventricular catheter and performed experiments on, *in vivo*, human brain tissue. In their study, the forces necessary to penetrate the brain ranged from 0.02 to 0.15 N, with an average of 0.08 N. Forces are influenced by the instruments' size and geometry of the tip [32, 33]. In [32], the authors investigated how the change in the shape and size of the probe tip would influence the magnitude of the force needed to insert the two cylindrical and one sharpened tip in a mouse brain. The resulting force ranges are from 0.32 to 1.61 N for the olfactory bulb insertion and from 0.51 to 2.48 N for the cortex insertion. One last strong example of instrumentation of surgical tool for evaluating the interaction forces during neurosurgery is the work of Rosen et al. [34]. In [34], the authors instrumented a laparoscopy grasper with a six DoF force/torque sensor, in order to check whether it was possible to evaluate surgeon skills from the interaction forces exerted to the tissue, using Markov models. In this study, they measured that novice surgeons exerted greater forces w.r.t. expert surgeons.

Even though several studies have already been proposed to measure the interaction forces during neurosurgery both *in vivo* and in vitro, to the best of our knowledge, an exhaustive study on the type of haptic feedback information in this context is still missing, especially regarding the cutaneous perception. On this regard, compared to the works presented above, our technique is superior, even if performed on a bench model, since (1) it considers three "realistic" scenarios, each of them corresponding to one tool; (2) its methodology is reproducible and repeatable, without constraints on the number of models that can be reproduced; (3) it employs more sensors—a load cell under the gelatin model and multiple 1-DoF contact force sensors on the tools; (4) it can be used to acquire several participants, without being restrained to the real operation.

The rest of paper is organized as follows. In Sect. 2, materials used, acquisition setup, and the experimental protocol are described. In Sect. 3, results are presented, whereas in Sect. 4 such results are discussed. In Sect. 5, conclusions are drawn, and future works are addressed.

2 Materials and methods

Our experimental setup was divided into two parts, one related to the contact force exerted to surgical tools and one concerning the interaction forces with the human brain phantom. Three neurosurgical tools were instrumented with 1-DoF contact force sensors and with passive retroreflective optical markers. Soft tissue mimicking material, replicating human brain tissue, was placed over a 3D printed plastic plate, rigidly fixed over a six DoF force/torque load cell, which measured force interactions between tool and tissue. The contact force sensors were connected to an acquisition board connected to a desktop PC (PC_1), whereas the load cell and the optical localization system were connected to a laptop workstation (PC_2). In what follows, a detailed description of the brain phantom, the used sensors, and the proposed methods is given.

2.1 Human brain replica and sensors

2.1.1 Human brain phantom

Parittotokkaporn et al. [35] suggested how to replicate the human brain tissue by using a mixture of gelatin and water. We replicated the human brain tissue mechanical proprieties with a mixture of gelatin and water, similarly to [35–37]. In particular, we used 7 % gelatin, shaping the resulting mixture as a solid uniform block. No tissue was applied, and no texture was replicated on the surface

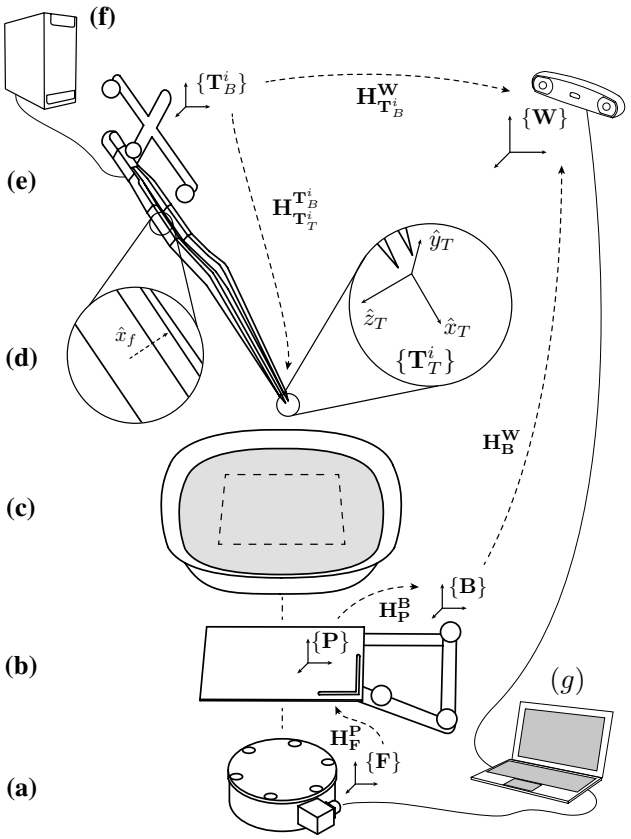

Fig. 1 Acquisition setup was composed by a (*c*) soft tissue mimicking phantom placed over a (*b*) Acrylonitrile Butadiene Styrene (ABS) 3D printed plate, fixed over a (*a*) six DoF force/torque load cell. The ABS 3D printed plate and each tool (*e*) were localized with passive retroreflective optical markers. Tools were instrumented with (*d*) contact force sensors, whereas the underlying load cell acquired the force exerted to the brain phantom. The (*f*) PC_1 was used for the contact force sensor measurement acquisition, while (*g*) PC_2 for the optical localization system and load cell measurement acquisition. Load cell reference frame {**F**}, ABS base reference frame {**P**}, ABS passive optical markers reference frame {**B**}, world reference frame {**W**} (which is also the optical localization system reference frame), *i*th tool passive optical markers reference frame $\{\mathbf{T}_B^i\}, i \in \mathbb{T}$, contact forces sensor reference axis $\hat{x}_f$, *i*th tool tip reference frame $\{\mathbf{T}_T^i\}$, and all the homogeneous transformation **H** are shown

of the phantom. The gelatin was stored in a refrigerator for at least eight hours before its usage. For each surgeon who performed the interaction tasks with the brain phantom, a new gelatin preparation was used, to avoid degradation of the shape and to standardize the response of the material. All the surgeons agreed that the brain phantom was in line with human brain consistency. The phantom was rigidly fixed to an Acrylonitrile Butadiene Styrene (ABS) plastic platform, depicted in Fig. 1b. The system composed by the box and the platform was placed over the load cell, depicted in Fig. 1a.

2.1.2 Contact force sensors

For measuring the contact forces exerted on the tools, we fixed Force Sensing Resistor™ (FSR™) sensors (400 and 408 series, Interlink Electronics Inc., Camarillo, CA, USA) on three neurosurgical tools, i.e., a bipolar forceps (BI), a spatula (SP), and a suction tool (SU). Surgeons were asked to held the bipolar forceps and the spatula between the thumb ($_T$) and the index finger ($_I$), whereas the suction tool had to be hold between the thumb, the index, and the middle finger ($_M$).

In detail (see Fig. 2),

- The bipolar forceps were instrumented with two FSR™408 sensors, one for the contact point of the thumb (BI_T) and one for the contact point of the index finger (BI_I). The bipolar forceps are commonly used in neurosurgery for safe and precise grasping and manipulating of tissue; in some medical context, e.g., electrosurgery, the bipolar forceps are also used to cut, coagulate, desiccate, or fulgurate tissue.
- The spatula was instrumented with three FSR™ 408 sensors, one for the contact point of the thumb (SP_T), one for the contact point of the index finger (SP_I), and one for a side of the tool, for a possible third contact point, (SP_S). The spatula is used for retracting and cutting brain tissue. In general, the tip of the spatula is bent in order to give the surgeon better maneuver abilities, without occluding the operation workspace.
- The suction tool was instrumented with three FSR™400 sensors, one for the contact point of the thumb (SU_T), one for the contact point of the index finger (SU_I), and one sensor for a third contact point on the tool (SU_M). The suction tool is used to destroy tissue and to aspirate excessive liquids.

We defined the tool set as $\mathbb{T} = \{BI, SP, SU\}$, and the contact force sensors set as $\mathbb{F} = \{\mathbb{F}_1 \cup \mathbb{F}_2 \cup \mathbb{F}_3\}$, where $\mathbb{F}_1 = \{BI_T, BI_I\}, \mathbb{F}_2 = \{SP_T, SP_I\}, \mathbb{F}_3 = \{SU_T, SU_I, SU_M\}$. Contacts at the SP_S sensor never occurred; thus, in the rest of the manuscript, it was considered not active.

Each contact force sensor mounted on the surgical tools has 1-DoF, i.e., $\hat{x}_f$ axis in Fig. 1d, and measures $f(t) \in \Re$, $t > 0$, that is, the amount of force applied by the surgeon's finger at the point where the sensor is attached. We are not interested in the orientation of the contact forces, but only at their magnitude. Therefore, in the rest of the manuscript, we will not consider the orientation of the $\hat{x}_f$ axes.

The tips of the bipolar forceps are two-pointed ends with a width of 10 mm, a height of 3 mm, and a thickness of 1.9 mm each. The tip of the spatula is rounded, with a width of 30 mm, a height of 12 mm, and a thickness of

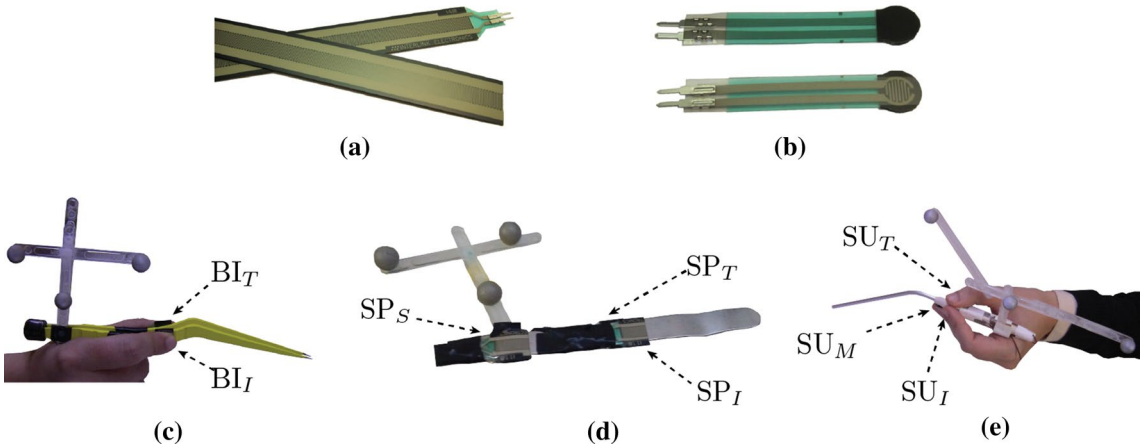

Fig. 2 *Upper row* Force-sensitive resistors fixed on the surgical tools, **a** FSR™ 408 series, **b** FSR™ 400 series. *Lower row* instrumented surgical tools, **c** bipolar forceps, **d** spatula, **e** suction tool. The contact force sensors are indicated by *dotted arrows*. BI_T and BI_I are the contact force sensors on the bipolar forceps at the contact points of the thumb and of the index, respectively. SP_T, SP_I, and SP_S are the contact force sensors on the spatula at the contact points of the *thumb*, of the *index*, and of the side sensor, in fact not active, respectively. SU_T, SU_I, and SU_M are the contact force sensors on the suction tool at the contact points of the *thumb*, of the *index*, and of the *middle finger*, respectively

2.3 mm. The tip of the suction tool is a cylindrical extremity, with a width of 30 mm and a radius of 2 mm.

FSR™ sensors come with a nominal thickness of 0.35–0.40 mm and a weight lower than 1 g, and does not affect the shape and the weight of the surgical tool once installed. For our application, we removed most of the sensor tip, which has a length of 622.3 mm, reducing the total length of the sensors to approximately 20 mm. The active area along the width dimension of the FSR™ 408 sensor strip is 5.08 mm; thus, we can estimate the maximal contact area to be 101.6 mm^2 (∼1 cm^2) for BI and SP. Since the contact areas on the suction tool are smaller than those on the other two tools, we installed on it three FSR™ 400 series sensors. The active area of one of these sensors is a circular section of radius 2.54 mm, resulting in a maximal contact area of 20.27 mm^2 (∼0.2 cm^2) for SU. Both series of FSR™ contact sensors have a full scale of 10 N, a resolution of 0.01 N. For the contact force value acquisition, we used a National Instruments DAQ acquisition board (National Instruments Corporation, Austin, TX, USA), which was connected to PC_1, running a customized Labview [38] interface. The sensor outputs were amplified by a standard operational amplifier TLO74CN, working as inverting configuration, with a reference voltage of 9 V. The acquisition frequency for the contact force sensors was set to 1000 Hz (see Sect. 2.2). To obtain force measurements from voltage values, a calibration of the FSR™ sensors was carried out by performing cycles of load/unload of known weights, from 10 to 350 g, and curve fitting on the acquired points. In the range 0–200 g, the calibration curve was considered linear ($R^2 = 0.99, RMSE = 8.862$ g).

2.1.3 Multi-axis load cell

For measuring the interaction forces between the tool and brain phantom, a six DoF Gamma Multi-Axis ATI force/torque Sensor (Gamma, ATI Industrial Automation, Apex, NC, USA) was placed under the soft tissue brain phantom box. The sensor has full scale of 32 N, resolution of 0.01 N, and sampling rate up to 7000 Hz. The load cell was connected to PC_2, a laptop workstation running an open real-time control framework OROCOS [39], for the acquisition of the force values.

We defined $\{\mathbf{F}\}$ as the load cell reference frame system, and we denoted force measurements in this reference frame system as $\mathbf{g}^{\{\mathbf{F}\}}(t) \in \Re^3$, $t > 0$. In this work, we are interested in the forces applied by the tools to the human brain replica; thus, we did not consider the torque components measured with the load cell. Consequently, resultant three-dimensional measurements are transformed onto the tool tip reference frame systems, and the first component, i.e., that in line with the main dimension of the tool, is selected (see Sect. 2.2 for details).

2.1.4 Optical localization system

In order to estimate the interaction force vector directed at each tool axis ($\hat{x}_T$ in Fig. 1), an NDI Polaris Vicra optical localization system (Northern Digital Inc., Waterloo, Canada) was used. The optical tracking system has an acquisition frequency of 20 Hz, with a static accuracy of 0.25 mm. A triad of passive retroreflective markers was fixed to each surgical tool, depicted in Fig. 1e, and to the ABS platform, depicted in Fig. 1b. The passive markers are visible in Fig. 2c–e. The

optical localization system was connected to PC_2, the same machine used for the acquisition of the load cell values.

2.2 Experimental protocol and data processing

2.2.1 Experimental protocol

Three neurosurgeons (S1–S3) performed interaction tasks with the brain phantom, while surgeon–tool contact forces and tool–tissue interaction forces measurements were collected. The three neurosurgeons defined the surgeons set $\mathbb{S}$. S3 has wide previous experience in neurosurgery, while S1 and S2 are completing neurosurgical training. The interaction list was designed with the help of an expert neurosurgeon, who did not participate to the data acquisition.

This research was conducted on healthy adult volunteers not paid for the participation. They were briefed about the task and its scope and afterward signed an informed consent, including the declaration of having no conflict of interest. All of them were able to give autonomously the consent. The experiment did not involve any collection of biological material or drug administration. The participation in the experiment did not involve the processing of genetic information or personal data (e.g., health, sexual lifestyle, ethnicity, political opinion, religious or philosophical conviction), neither the tracking of the location nor observation of the participants. Our organizations do not require any IRB review for cases like the one scope of this study.

The interaction list, equal for all the participants, was composed of the following eight tasks, each taken three times, sorted in a pseudo-random order:

1. Texture test with bipolar forceps (BiC): The user touches the brain phantom surface with the tool tips slightly opened, having care to not penetrate the material.
2. Penetration test with bipolar forceps (BiP): The user places the tool tips slightly opened on the surface of the brain phantom and then gently enter in it. The tool tip has to enter for approximately 10 mm, i.e., the uncovered portion of tool tip. The task is over when the user exits the material, by following the same direction of entrance.
3. Grab test with bipolar forceps (BiG): The user enters the soft tissue mimicking material for approximately 10 mm, keeping the tool tips opened. Then, the user simulates a grasp and eventually exit the material keeping the tool closed.
4. Texture test with spatula (SpC): The user touches the brain phantom with the tool tip, having care to not enter inside the material.
5. Cut test with spatula (SpK): The user enters the brain phantom for approximately 20 mm with the tool tip, cutting the surface. Then, the user exits following the same direction along which the tool was inserted.
6. Displacement test with spatula (SpD): The user inserts the tool tip inside one of the cuts previously done with the cut task. Once the tool is inside, the user displaces part of the material, simulating the intention to look inside the displaced part. Then, the user pulls out the tool from the material, following a direction perpendicular to the tissue surface. In the interaction list, the task SpD always came after the task SpK.
7. Texture test with suction tool (SuC): The user touched the brain phantom with the tool tip, having care to not enter inside the material.
8. Penetration test with suction tool (SuP): The user penetrates the brain phantom for approximately 20 mm with the tool tip. Then, the user exits from the material by the same direction along which the tool was inserted.

The eight tasks defined the task set $\mathbb{K} = \{\mathbb{K}_1 \cup \mathbb{K}_2 \cup \mathbb{K}_3\}$, where $\mathbb{K}_1 = \{BiC, BiP, BiG\}, \mathbb{K}_2 = \{\text{SpC}, \text{SpK}, \text{SpD}\}$, and $\mathbb{K}_3 = \{\text{SuC}, \text{SuP}\}$.

Each element of the interaction list was performed four times, $N = 4$, interacting with the brain phantom along the borders of an abstract square placed over the tissue (see Fig. 1c). The interaction list included 24 tasks, resulting in 96 trials per surgeon.

During the trials, surgeons were asked to perform the tasks as natural as possible, with no requirements on completion time. However, surgeons were asked to avoid touching the gelatin container, since such contacts invalidate the load cell measurements, since a contact with the container implies that the simulation does not include only the brain tissue but also the skull.

Remark Texture test tasks, i.e., BiC, SpC, and SuC, are motivated by the fact that some neurosurgery procedures require surgical tools to be in contact with the brain tissue. A particularly clear example is the cortical stimulation mapping procedure, in which the tool, i.e., the electrode, is placed on the brain at specific different brain sites, to test motor, sensory, language, or visual functions. Still regarding these tasks, even if no specifications on applied forces were given, surgeons were asked to not penetrate the tissue.

Remark In the penetration tasks, i.e., BiP, SpK, and SuP, specifying a fixed penetration length permitted us to uniform different surgeons' behaviors, so that penetrations by different surgeons were performed in same way.

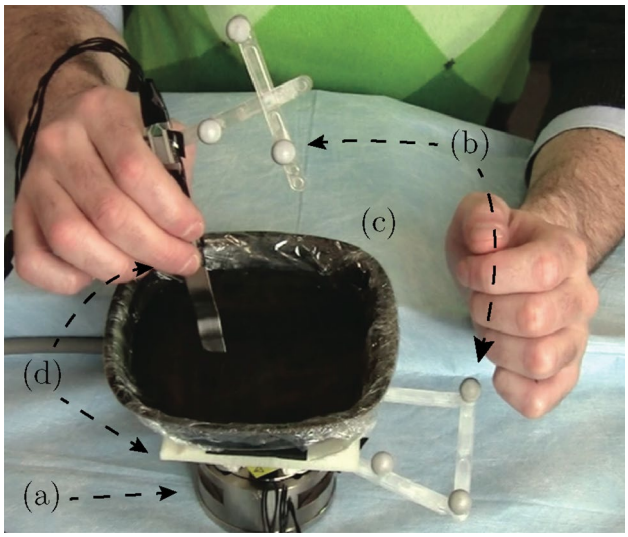

Fig. 3 Setup for interaction force acquisition. The surgeon is performing the cut test with spatula (SpK). The (*a*) multi-axis load cell, the (*b*) passive optical markers on the tool and on the ABS plate base, and (*c*) the brain phantom are visible, whereas the (*d*) ABS plate and the contact force sensors are partially occluded

Each task in the interaction list was composed by three consequential phases: synchronization, interaction, and resting phase [see Fig. 4a, b, (1–3)]. During the synchronization phase, the surgeon approached the acquisition setup, in comfortable position (see Fig. 3), the brain phantom box was fixed over the ABS plate, the load cell was reset, and the surgeon produced a force spike on one of the contact sensors of the tool in use, while the tool itself was lying on the gelatin container above the load cell. This force spike was measured both by the contact sensor and the load cell, and it was used to off-line synchronize the stream of signals recorded, by aligning the two spikes. Examples of force spikes are visible in Fig. 4a, b, 1. In the subsequent interaction phase, the surgeon executed N times the current task. In the resting phase, the surgeon was free to leave the acquisition set, and the data recording was stopped.

2.2.2 *Data processing*

Each sensor used in the data acquisition has its own sampling rate. The load cell can stream data through ethernet connection up to 7000 Hz, the optical localization system runs at 20 Hz, whereas the sampling rate of the contact force sensors depend on the acquisition board setup. We uniformed the sampling rates by setting the operational frequency of the acquisition setup to 1000 Hz and then by down-sampling the load cell frequency to 1000 Hz and by over-sampling the optical localization system to 1000 Hz.

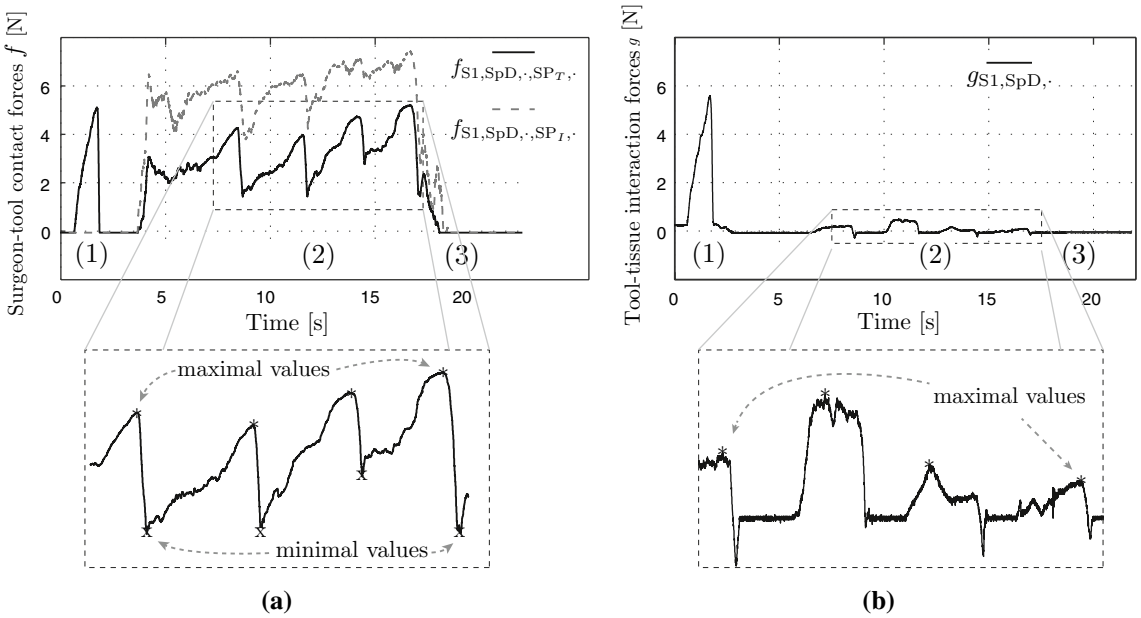

Fig. 4 Example of displacement test with spatula (SpD) performed by S1. **a** *upper figure* surgeon–tool contact forces measured by the contact sensors continuous and *dotted lines* represent the thumb $f_{S1,SpD,\cdot,SP_T,\cdot}$ and the *index* sensor $f_{S1,SpD,\cdot,SP_I,\cdot}$ measurements. **a** *lower figure* magnification of **a** *upper figure* interaction phase, *stars* and *crosses* represent the maxima and the minima selected in the trial, respectively. **b** Tool–tissue interaction forces measured by the load cell: the continuous line represents the measurements of the tool–tissue interaction forces g along the $\hat{x}_T$ axis of the spatula tool. **b** *Lower figure* magnification of **b** *upper figure* interaction phase, *stars* represent the maxima selected in the trial. Both figures: (*1*) synchronization phase, (*2*) interaction phase, (*3*) resting phase. In (*1*), force spikes used for the off-line synchronization of the signals are visible

With this choice, we aim to avoid any possible contact sensor measurements loss, by keeping high-frequency components of the contact forces, at the cost of having several replicated measurements for the localization system. In fact, this choice is equivalent to the assumption that the tools do not move more than 0.25 mm in a time range of 50 ms, for all the trials, i.e., the velocity of each tool is always lower than 5 mm/s. Eventually, for each performed trial, a synchronization step was needed, as previously described for the synchronization phase of a task.

In order to transform force measurements acquired by the load cell onto the tool tips reference frame systems, we firstly defined

- $\{\mathbf{W}\}$ as the world reference frame, represented by the optical localization system base frame,
- $\{\mathbf{P}\}$ as the reference frame of the ABS plate,
- $\{\mathbf{B}\}$ as the reference frame of the passive optical retroreflective markers attached to the ABS plate,
- $\{\mathbf{T}_B^i\}$ as the reference frame of the passive optical retroreflective markers attached to the ith surgical tool, $i \in \mathbb{T}$,
- $\{\mathbf{T}_T^i\}$ as the ith surgical tool tip reference frame, and
- $\mathbf{H}_{\mathbf{F}}^{\mathbf{P}} \in \Re^{4\times4}$ as the rigid homogeneous transformation between $\{\mathbf{P}\}$ and $\{\mathbf{F}\}$, computed using the CAD model of the ABS plate,
- $\mathbf{H}_{\mathbf{P}}^{\mathbf{B}} \in \Re^{4\times4}$ as the rigid homogeneous transformation between $\{\mathbf{B}\}$ and $\{\mathbf{P}\}$, computed using a pivoting procedure,
- $\mathbf{H}_{\mathbf{B}}^{\mathbf{W}} \in \Re^{4\times4}$ as the rigid homogeneous transformation between $\{\mathbf{W}\}$ and $\{\mathbf{B}\}$, computed using the optical localization system,
- $\mathbf{H}_{\mathbf{T}_B^i}^{\mathbf{W}} \in \Re^{4\times4}$ as the rigid homogeneous transformation between $\{\mathbf{W}\}$ and $\{\mathbf{T}_B^i\}$, computed using the optical localization system, depending on the time, and
- $\mathbf{H}_{\mathbf{T}_T^i}^{\mathbf{T}_B^i} \in \Re^{4\times4}$ as the rigid homogeneous transformation between $\{\mathbf{T}_B^i\}$ and $\{\mathbf{T}_T^i\}$, computed using a pivoting procedure.

Reference systems are shown in Fig. 1.

Then, for each task j in the interaction list and for each surgeon s, the measured contact forces are specified as $f_{s,k,j,c}(t) \in \Re$, $t > 0$, where $c \in \mathbb{F}$ are the contact force sensors considered in the task, $s \in \mathbb{S}$, $k \in \mathbb{K}$ is the type of task performed, $i \in \mathbb{T}$ is the and $j = 1, \ldots, 24$. In each task, only the relevant contact forces sensors measurements were recorded.

Using the notation just introduced, we specify the measurements applied by the ith tool, $i \in \mathbb{T}$, to the load cell w.r.t. the tool tip reference frame $\{\mathbf{T}_T^i\}$, $\mathbf{g}_{s,k,j,c}^{\{\mathbf{T}_T^i\}}(t) \in \Re^3$, $t > 0$, as

$$\begin{bmatrix} \mathbf{g}_{s,k,j}^{\{\mathbf{T}_T^i\}}(t) \\ 1 \end{bmatrix} = \mathbf{H}_{\mathbf{F}}^{\mathbf{T}_T^i} \begin{bmatrix} \mathbf{g}_{s,k,j}^{\{\mathbf{F}\}}(t) \\ 1 \end{bmatrix}, \quad t > 0$$

where

$$\mathbf{H}_{\mathbf{F}}^{\mathbf{T}_T^i} = \mathbf{H}_{\mathbf{T}_B^i}^{\mathbf{T}_T^i}\, \mathbf{H}_{\mathbf{W}}^{\mathbf{T}_B^i}(t)\, \mathbf{H}_{\mathbf{B}}^{\mathbf{W}}\, \mathbf{H}_{\mathbf{P}}^{\mathbf{B}}\, \mathbf{H}_{\mathbf{F}}^{\mathbf{P}},$$

$$\mathbf{H}_{\mathbf{W}}^{\mathbf{T}_B^i} = \left(\mathbf{H}_{\mathbf{T}_B^i}^{\mathbf{W}}\right)^{-1},$$

and where $s \in \mathbb{S}, k \in \mathbb{K}, j = 1, \ldots, 24$, and $(\cdot)^{-1}$ the inverse operator.

The rigidity of the materials between the gelatin and the load cell, i.e., the ABS base (see Fig. 1b) and the gelatin container (see Fig. 1c), permits to assume that the tool–tissue interaction forces at the tool tip $\mathbf{g}_{s,k,j}^{\{\mathbf{T}_T^i\}}(t)$ can be directly determined via a transformation of the force measurements acquired by the load cell $\mathbf{g}_{s,k,j}^{\{\mathbf{F}\}}(t)$.

We were interested in the $\hat{x}_T$ axis of the tool tip reference frame, that is, the first component of $\mathbf{g}^{\{\mathbf{T}_T^i\}}$. Therefore, in the following, we considered only these first components, denoted as $g_{s,k,j}(t) \in \Re$, $t > 0$ (following the above-introduced notation), and referred to as "tool–tissue interaction forces."

We manually selected, for each task j in the interaction list of each surgeon s,

- four maximal values for each relevant contact force sensor, $f_{s,k,j,c,n}^{max}$
- four minimal values for each relevant contact force sensor, $f_{s,k,j,c,n}^{min}$
- four maximal values from the load cell measurements, $g_{s,k,j,n}^{max}$

where $j = 1, \ldots, 24, c \in \mathbb{F}$, and $n = 1, \ldots, 4$.

Only the relevant contact force sensors were considered: $c \in \mathbb{F}_1$ for the bipolar forces, $c \in \mathbb{F}_2$ for the spatula, and $\in \mathbb{F}_3$ for the suction tool. Moreover, S1 never stimulated the contact sensor SU_I while S2 and S3 did not apply forces on SU_M. Therefore, we combined values from these two sensors in a single sensor data measurements, which was referred to as SU_{M-I} in the following.

Consequently, we specified the "surgeon–tool contact forces" as

$$\tilde{f}_{s,k,j,c,n} = f_{s,k,j,c,n}^{max} - f_{s,k,j,c,n}^{min} \tag{1}$$

where $k \in \mathbb{K}, s \in \mathbb{S}, c \in \mathbb{F}, j = 1, \ldots, 24$, and $n = 1, \ldots, 4$. Since each neurosurgeon performed 96 trials, we collected 288 measurements per surgeon, having three values per trial, i.e., two FSR™ sensors for the contact forces and one load cell for the brain tissue forces, with a total amount of 864 measurements.

In order to compare the performances of the three surgeons, Kruskal–Wallis tests (α level of 0.05, Bonferroni correction) and multiple comparison procedures as follow-up test were performed on surgeon–tool contact forces and tool–tissue interaction forces.

3 Results

Surgeon–tool contact forces Figure 5a shows measurements of the surgeon–tool contact forces, computed using (1) at the thumb (left columns), and at the index and middle finger (right columns), expressed in N, collected by tasks. As far as the thumb contact is concerned (left columns, Fig. 5a), all the surgeons behaved similarly within a forces range of 0.01–3 N, with only one exception for the spatula task SpD reaching 3.49 N. As far as the index and middle finger contacts are concerned (right columns, Fig. 5a), we can highlight that for the task concerning the bipolar forceps, the three surgeons seldom exerted forces greater than 1 N. A similar consideration can be made for the suction tool, for which the surgeons did not exert forces greater than 3 N. Exceptions to these force ranges are tasks performed with the spatula. Although median values belonging to these measurements are similar to those measured with the other tools, surgeons did exert greater forces with this tool, with a maximum value reaching a peak of 6.6 N. Significant differences among the medians of the thumb contact sensor and the index–middle finger contact sensor were found in the task SuP ($p < 0.025$).

Tool–tissue interaction forces Figure 5b shows the values for the measured tool–tissue interaction forces, expressed in N, collected by tasks. For the texture tasks, i.e., BiC, SpC, and SuC, we can note that the values of the measured forces are rarely higher than 0.1 N. In fact, these tasks are trivial touches of the brain phantom; thus, this behavior was expected. Greater forces were detected during the other tasks, especially during penetration tasks such as SpK and SuP. For these interactions, we measured the maximum force values, with the highest value of 0.59 N. Significant differences between medians were found for the three tasks with the spatula and for the two tasks with the suction tool.

4 Discussion

In this work, we measured the interaction forces between neurosurgeons and surgical tools (surgeon–tool contact forces) and between surgical tools and a brain phantom (tool–tissue interaction forces), during cutting and penetration tasks. Table 1 summarizes our collected measurements, and it presents range comparisons between our data and the closest works in the literature.

As a general result, the tool–tissue interaction forces were very low w.r.t to those measured by the contact force sensors. For the sensors activated by the thumb, i.e., $\mathrm{BI}_T, \mathrm{SP}_T$, and SU_T, the surgeon–tool contact forces were up to around six times higher than what applied to the brain phantom (first row of Table 1a over first row of Table 1b). For the sensors activated by the index and middle finger, i.e., $\mathrm{BI}_I, \mathrm{SP}_I$, and SU_{M-I}, the surgeon–tool contact forces were up to around 11 times higher than the tool–tissue interaction forces (second row of Table 1a over first row of Table 1b).

Although we used a bench model for simulating the interaction between the surgical tools and the brain tissue, our load cell measurements are justified by the model of the brain phantom we used, and by force measurements obtained by studies on real tele-operated and non-operations, present in the literature.

The brain phantom we used in this work was already proposed in the literature [35, 37], and the neurosurgeons who participated at our acquisition agreed that its texture was similar to the one of in vivo brain tissue. In this regard, Gefen et al. [40] showed that the mechanical characteristics of brain tissue were statistically indistinguishable *in vivo* and *in vitro*. Thus, our results are comparable with *in vitro* acquisitions.

In [29], the authors presented force measurements on cadaver brain tissue, and they reported median force values between 0.00 and 0.18 N when interacting with cerebrum tissue using a spatula (second row of Table 1b). The authors used a six DoF force/torque sensor, but we assume that the reported force values are computed as the Euclidean norm of the solely force components. Maddahi et al. [30] measured the interaction forces during four robot-assisted neurosurgical operations. The authors employed a bipolar force and a suction tool, linked to the robot end-effector via two six DoF force/torque sensors. Regarding the interaction forces applied by the robot end-effectors to the brain tissues, the authors measured maximum force of 1.86 N, with mean values of $0.38\,\mathrm{N} \pm 0.05\,\mathrm{N}$ for the bipolar forceps and $0.21\,\mathrm{N} \pm 0.03\,\mathrm{N}$ for the suction tool. Howard et al. [31] measured a similar force range (0.02–0.15 N) when penetrating in vivo brain tissue with a standard ventricular catheter (third row of Table 1b). Sharp et al. [32] measured how the shape and the size of probes influence the force needed for inserting cylindrical and sharpened tips in a mouse brain. The resulting force ranges were from 0.32 to 1.61 N and 0.51 to 2.48 N, for olfactory bulb and cortex insertion, respectively (fourth row of Table 1b). All four works [29–32] presented procedures similar to our. Nevertheless, they did not consider the haptic perception at the surgeon's fingertip, focusing only on forces applied to

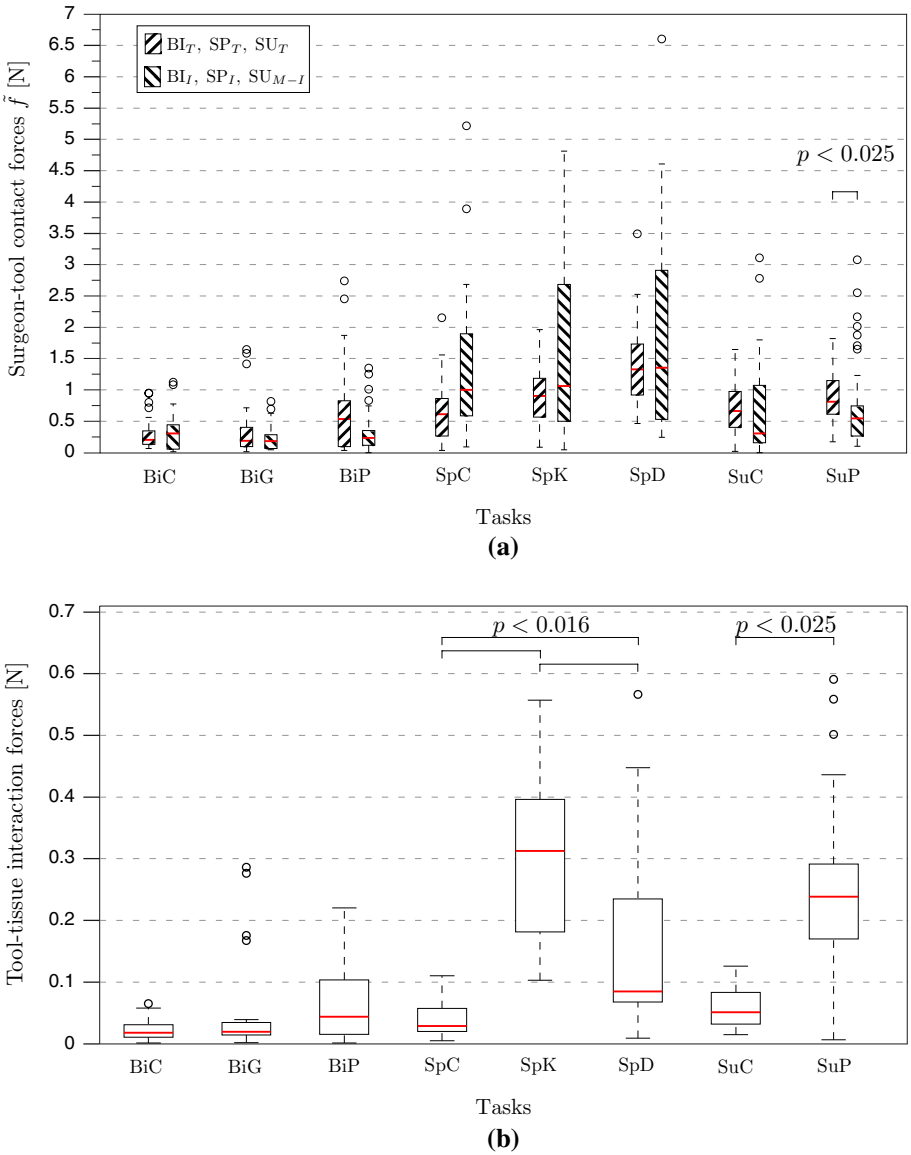

Fig. 5 Surgeon–tool contact forces and tool–tissue interaction forces: **a** measurements from the contact force sensors pressed by the thumb, i.e., BI_T, SP_T, and SU_T, and by the index and middle fingers, i.e., BI_I, SP_I, and SU_{M-I}, expressed in N, collected by tasks; **b** measurements from the load cell, expressed in N, collected by tasks. Both figures: for each task, the medians, the 25th and the 75th percentiles of the samples, the whiskers for the minimal and maximal values are shown. Outliers are depicted with *circles*. Significant differences between medians are marked with *horizontal brackets*

cadaver [29], mouse brain [31], and *in vivo* tissue [30, 32]. Eventually, the interaction force values presented by these works are in line with our acquisition, especially when considering median values (see red dashes in Fig. 5b). For this reason, we believe that our results have an application for what concern the haptic rendering in tele-operated robotic surgery.

Moreover, when compared to a real operation data measurements, our bench model has several strengths: (1) possibility to repeat the performed trials on customizable brain phantoms, which is not possible for real surgery; (2) very accurate measurements of the tool–tissue interaction forces, thanks to the load cell placed under our brain phantom container—which in real operations is not possible to place; (3) very accurate measurements of the surgeon–tool contact forces, which due to the lightweight propriety of the contact sensors, are really faithful to those in play when no sensor is mounted on the tool.

As far as tool–tissue interaction forces are concerned, when using the bipolar gripper, all three surgeons perceived up to 0.5 N on the contact forces on the thumb and the index, while tool–tissue interaction forces were less than 0.05 N, which is around the minimal threshold for the kinesthetic perception [18] (see Table 1a). When using the spatula, tool–tissue interaction forces were greater and well above the sensitivity thresholds for kinesthetic feedback, whereas for the suction tool kinesthetic perception was above threshold in case of penetration, while cutting resistance was too small to be perceived.

As far as contact forces are concerned, each surgeon behaved similarly, and differences were due to the particular chosen grip. Since each surgeon has a slightly different grip

Table 1 Measured surgeon–tool contact forces and tool–tissue interaction forces

Measured surgeon–tool contact forces and finger pad sensitivity ranges[a]	
	Range (N)
Surgeon–tool contact forces—thumb	0.01–3.49
Surgeon–tool contact forces—index–middle f.	0.01–6.6
Human finger pad sensitivity—Lederman, [13]	0.05–3.5
Measured tool–tissue interaction forces and relevant works force ranges[b]	
	Range (N)
Tool–tissue interaction forces	0.01–0.59
Marcus et al. [29]	0.00–0.18[c]
Maddahi et al. [30]	0.38 ± 0.05[d]
	0.21 ± 0.03[e]
Howard et al. [31]	0.02–0.15
Sharp et al. [32][h]	0.32–1.61[f]
	0.51–2.48[g]

[a] Comparison of the surgeon–tool contact forces with human finger pad sensitivity (Lederman, [13])

[b] Comparison tool–tissue interaction forces with related works in literature (Marcus et al. [29]; Maddahi et al. [30]; Howard et al. [31]; Sharp et al. [32])

[c] Interaction with cerebrum tissue.

[d] Bipolar forceps.

[e] Suction tool.

[f] Performed on a mouse brain.

[g] Olfactory bulb insertion.

[h] Cortex insertion

of the tool, different positions of the sensors would have been needed for each different person. Determining the best measurements for the interaction forces bring some criticisms. Also, the experience and the different training duration of a surgeon strongly influence the way she/he grips the tool. We fixed the position of the contact sensors and asked the surgeons to hold the tool in the way we specified.

The aim of this work was to check whether the interaction forces during a bench model neurosurgery operation would be small enough to lie in the solely cutaneous perception of the human finger pads. This would enable the use of sensory subtraction techniques for providing surgeons with feedback from neurosurgical operations.

In our acquisition, we measured surgeon–tool contact forces in a range 0.01–3.49 N for sensors pressed by the thumb, and in a range 0.01–6.6 N for sensors stimulated by the index and the middle finger. Although median values belonging to these measurements are similar to those measured with the other tools, surgeons did exert greater forces with the spatula, with a maximum value reaching a peak of 6.6 N. Significant differences among the medians of the thumb contact sensor and the index–middle finger contact sensor were found in the penetration task with the spatula ($p < 0.025$).

Since our results fit the sensitivity range of the finger pad characterized by Lederman [13] (see Table 1a)—with few exceptions coming from the tasks performed with the spatula—we deem that our work has reached its aim. This means that the surgeon–tool contact forces meet the requirements for the use of sensory subtraction techniques [23, 24] in a tele-operated robotic neurosurgery scenario. This kind of forces can be rendered by exploiting the solely surgeon's finger pads cutaneous channel, since it comprises forces that are lower than the threshold from which the haptic perception switches from the cutaneous to the kinesthetic channel. A tele-operated neurosurgery system in which the haptic feedback is given to the operator by means of sensory substitution techniques would be highly transparent and it would be more stable than one where the complete haptic feedback is provided. However, the present study is intended to be just a preliminary step on the feasibility of this approach. The applicability of these techniques in a tele-operated robotic neurosurgery context is in the scope of future works.

5 Conclusion

In this paper, we analyzed whether the forces exerted on tools by surgeons performing neurosurgery would be small enough so that sensory subtraction techniques could be valid and useful in a tele-operated robotic neurosurgery scenario. Measured forces are lower than 3.5 N, with few exceptions and can be rendered by conveying haptic cues just through the cutaneous channel of surgeon's finger pads, thus skipping the kinesthetic component of the haptic feedback. Tool–tissue interaction forces are in general lower than 0.4–0.5 N, with few exceptions, and in line with the relevant literature. A tele-operated neurosurgery system designed on this base would be highly transparent, and it would be more stable than those systems where a complete haptic feedback is provided. Improvements to this work can be achieved by exploiting the robotic grasp theory into the surgeon–tool contact forces analysis [41], i.e., by mathematical modeling of the tools and the surgeons' fingers. In this way, we think we can improve the insight on the contact force information at the fingertip level.

Acknowledgments The authors acknowledge the contribution of Danilo De Lorenzo for his assistance with the acquisition setup. The research leading to these results has received funding from the European Union Seventh Framework Programme FP7/2007–2013 under Grant Agreement No. 270460 of the project "ACTIVE: Active Constraints Technologies for Ill defined or Volatile Environment" and under Grant agreement No. 601165 of the project "WEARHAP—WEARable HAPtics for humans and robots."

Compliance with ethical standards

Conflict of interest The authors declare that they have no conflict of interest.

References

1. Salisbury K, Conti F, Barbagli F (2004) Haptic rendering: introductory concepts. IEEE Comput Graphics Appl 24(2):24–32
2. Salcudean S, Ku S, Bell G (1997) Performance measurement in scaled teleoperation for microsurgery, in *CVRMed-MRCAS'97*. Springer, pp. 789–798
3. De Lorenzo D, De Momi E, Conti L, Votta E, Riva M, Fava E, Bello L, Ferrigno G (2013) Intraoperative forces and moments analysis on patient head clamp during awake brain surgery. Med Biol Eng Comput 51(3):331–341
4. De Lorenzo D, De Momi E, Dyagilev I, Manganelli R, Formaglio A, Prattichizzo D, Shoham M, Ferrigno G (2011) Force feedback in a piezoelectric linear actuator for neurosurgery. Int J Med Robot Comput Assist Surg 7(3):268–275
5. De Lorenzo D, Koseki Y, De Momi E, Chinzei K, Okamura A (2013) Coaxial needle insertion assistant with enhanced force feedback. IEEE Trans Biomed Eng 60(2):379–389
6. Massimino M, Sheridan T (1994) Teleoperator performance with varying force and visual feedback. Hum Factors J Hum Factors Ergon Soc 36(1):145–157
7. Moody L, Baber C, Arvanitis TN et al (2002) Objective surgical performance evaluation based on haptic feedback. Stud Health Technol Inf 85(2):304–310
8. Wagner C, Stylopoulos N, Howe R (2002) The role of force feedback in surgery: analysis of blunt dissection. In: Symposium on haptic interfaces for virtual environment and teleoperator systems, Citeseer, pp 73–79
9. Lang M, Sutherland G (2010) Informatic surgery: the union of surgeon and machine. World Neurosurg 74(1):118–120
10. Guidali M, Duschau-Wicke A, Broggi S, Klamroth-Marganska V, Nef T, Riener R (2011) A robotic system to train activities of daily living in a virtual environment. Med Biol Eng Comput 49(10):1213–1223
11. Ellis R, Ismaeil O, Lipsett M (1996) Design and evaluation of a high-performance haptic interface. Robotica 14(03):321–327
12. Okamura AM (2004) Methods for haptic feedback in teleoperated robot-assisted surgery. Ind Robot Int J 31(6):499–508
13. Lederman S (1991) Skin and touch. Encycl Hum Biol 7:51–63
14. Sherrick C, Craig J (1982) The psychophysics of touch: a sourcebook. Tactual perception, p 55
15. Goethals P (2008) Tactile feedback for robot assisted minimally invasive surgery: an overview. In: Internal Report, Department of Mechanical Engineering KU Leuven
16. Sherrick C, Cholewiak RW (1986) Cutaneous sensitivity. Handb Percept Hum Perform 1:1–12
17. Hale K, Stanney K (2004) Deriving haptic design guidelines from human physiological, psychophysical, and neurological foundations. IEEE Comput Graphics Appl 24(2):33–39
18. Jones L (2000) Kinesthetic sensing. In: Human and machine haptics. MIT Press
19. Hashtrudi-Zaad K, Salcudean S (2002) Transparency in time-delayed systems and the effect of local force feedback for transparent teleoperation. IEEE Trans Robot Autom 18(1):108–114
20. Franken M, Stramigioli S, Misra S, Secchi C, Macchelli A (2011) Bilateral telemanipulation with time delays: a two-layer approach combining passivity and transparency. IEEE Trans Robot 27(4):741–756
21. Bach-y Rim P, Webster J, Tompkins W, Crabb T (1987) Sensory substitution for space gloves and for space robots. In: Proceedings IEEE international conference on robotics and automation, vol 2. ICRA, pp 51–57
22. Massimino M (1995) Improved force perception through sensory substitution. Control Eng Pract 3(2):215–222
23. Prattichizzo D, Pacchierotti C, Rosati G (2012) Cutaneous force feedback as a sensory subtraction technique in haptics. IEEE Trans Haptics 5(4):289–300
24. Pacchierotti C, Tirmizi A, Prattichizzo D (2013) Improving transparency in eleoperation by means of cutaneous tactile force feedback. ACM Trans Appl Percept 11:4
25. Mihelj M, Podobnik J (2012) Haptic displays. In: Haptics for virtual reality and teleoperation, Series Intelligent Systems, Control and Automation: Science and Engineering, vol 64. Springer, Netherlands, pp 57–73
26. Miller K, Chinzei K, Orssengo G, Bednarz P (2000) Mechanical properties of brain tissue in-vivo: experiment and computer simulation. J Biomech 33(11):1369–1376
27. Sutherland G, Wolfsberger S, Lama S, Zarei-nia K (2013) The evolution of neuroArm. Neurosurgery 72:A27–A32
28. Chen Z, Gillies G, Broaddus W, Prabhu S, Fillmore H, Mitchell R, Corwin F, Fatouros P (2004) A realistic brain tissue phantom for intraparenchymal infusion studies. J Neurosurg 101(2):314–322
29. Marcus H, Zareinia K, Gan L, Yang F, Lama S, Yang G-Z, Sutherland G (2014) Forces exerted during microneurosurgery: a cadaver study. Int J Med Robot Comput Assist Surg 10(2):251–256
30. Maddahi Y, Gan LS, Zareinia K, Lama S, Sepehri N, Sutherland G (2015) Quantifying workspace and forces of surgical dissection during robot-assisted neurosurgery. Int J Med Robot Comput Assist Surg
31. Howard M III, Abkes B, Ollendieck M, Noh M, Ritter R, Gillies G (1999) Measurement of the force required to move a neurosurgical probe through in vivo human brain tissue. IEEE Trans Biomed Eng 46(7):891–894
32. Sharp A, Ortega A, Restrepo D, Curran-Everett D, Gall K (2009) In vivo penetration mechanics and mechanical properties of mouse brain tissue at micrometer scales. IEEE Trans Biomed Eng 56(1):45–53
33. Jensen W, Yoshida K, Hofmann U (2006) In-vivo implant mechanics of flexible, silicon-based acreo microelectrode arrays in rat cerebral cortex. IEEE Trans Biomed Eng 53(5):934–940
34. Rosen J, Hannaford B, Richards CG, Sinanan MN (2001) Markov modeling of minimally invasive surgery based on tool/tissue interaction and force/torque signatures for evaluating surgical skills. IEEE Trans Biomed Eng 48(5):579–591
35. Parittotokkaporn T, Frasson L, Schneider A, Huq S, Davies BL, Degenaar P, Biesenack J, Rodriguez y Baena F (2009) Soft tissue traversal with zero net force: feasibility study of a biologically inspired design based on reciprocal motion. In: IEEE international conference on robotics and biomimetics, ROBIO. IEEE, pp 80–85
36. Ritter RC, Quate E, Gillies G, Grady M, Howard IMA, Broaddus W (1998) Measurement of friction on straight catheters in in vitro brain and phantom material. IEEE Trans Biomed Eng 45(4):476–485
37. De Lorenzo D, Manganelli R, Dyagilev I, Formaglio A, De Momi E, Prattichizzo D, Shoham M, Ferrigno G (2010) Miniaturized rigid probe driver with haptic loop control for neurosurgical interventions. In: Proceedings IEEE-RAS EMBS international conference on biomedical robotics and biomechatronics, BioRob. IEEE, pp 522–527
38. LabVIEW System Design Software, National Instruments Corporation. http://www.ni.com/labview/
39. The OROCOS Project. http://www.orocos.org/
40. Gefen A, Margulies S (2004) Are in vivo and in situ brain tissues mechanically similar? J Biomech 37(9):1339–1352

41. Prattichizzo D, Trinkle JC (2008) Grasping. In: Springer handbook of robotics. Springer, pp 671–700

Marco Aggravi (M.E. Computer Engineering, 2011, University of Siena) is currently Ph.D. Student at the Siena Robotics and Systems lab (SIRSlab), DIISM, University of Siena.

Elena De Momi (M.Sc. Biomedical Engineering, 2002, Ph.D. Bioengineering, 2006, Politecnico di Milano) is an Assistant Professor at the DEIB, Politecnico di Milano, Milano, Italy.

Francesco DiMeco is a neurosurgeon, Primary, and Director at the Department of Neurosurgery at the "Fondazione Istituto Neurologico C. Besta" of Milan, Italy.

Francesco Cardinale is a neurosurgeon at the "Claudio Munari" Epilepsy and Parkinson Surgery Centre of the Niguarda Hospital, in Milan, Italy.

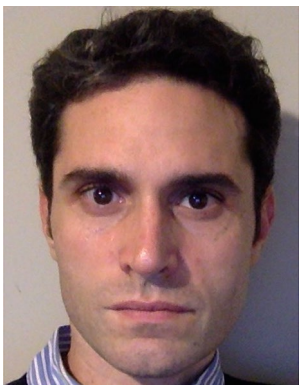

Giuseppe Casaceli is a neurosurgeon at the "Claudio Munari" Epilepsy and Parkinson Surgery Centre of the Niguarda Hospital, in Milan, Italy.

Marco Riva is a neurosurgeon at the Oncological Neurosurgery Unit of the Humanitas Research Hospital. He is also a visiting scholar at the IUSS Center for Neurocognition, Epistemology and Theoretical Syntax.

Giancarlo Ferrigno (M.Sc. Electrical Engineering, 1983, Ph.D. Bioengineering, 1990, Politecnico di Milano) is currently a Full Professor at the DEIB and Director at the NEARLab, Politecnico di Milano, Milano, Italy.

Domenico Prattichizzo (M. Sc. Electronics Engineering, 1991, Ph.D. Robotics and Automation, 1995, University of Pisa) is currently a Full Professor at the DIISM, University of Siena.